

Springtime CO₂ exchange over seasonal sea ice in the Canadian Arctic Archipelago

Tim PAPAKYRIAKOU,¹ Lisa MILLER²

¹Centre for Earth Observation Science, Department of Environment and Geography, University of Manitoba, 470 Wallace Bldg, 125 Dysart Road, Winnipeg, Manitoba R3T 2N2, Canada

E-mail: papakyri@cc.umanitoba.ca

²Institute of Ocean Sciences, Fisheries and Oceans Canada, Sidney, British Columbia V8L 4B2, Canada

ABSTRACT. Springtime measurements of CO₂ exchange over seasonal sea ice in the Canadian Arctic Archipelago using eddy covariance show that CO₂ was generally released to the atmosphere during the cold (ice surface temperatures less than about -6°C) early part of the season, but was absorbed from the atmosphere as warming advanced. Hourly maximum efflux and uptake rates approached 1.0 and $-3.0\ \mu\text{mol m}^{-2}\text{s}^{-1}$, respectively. These CO₂ flux rates are far greater than previously reported over sea ice and are comparable in magnitude to exchanges observed within other systems (terrestrial and marine). Uptake generally occurred for wind speeds in excess of $6\ \text{m s}^{-1}$ and corresponded to local maxima in temperature at the snow–ice interface and net radiation. Efflux, on the other hand, occurred under weaker wind speeds and periods of local minima in temperature and net radiation. The wind speeds associated with uptake are above a critical threshold for drifting and blowing snow, suggesting that ventilation of the snowpack and turbulent exchange with the brine-wetted grains are an important part of the process. Both the uptake and release fluxes may be at least partially driven by the temperature sensitivity of the carbonate system speciation in the brine-wetted snow base and upper sea ice. The period of maximum springtime CO₂ uptake occurred as the sea-ice permeability increased, passing a critical threshold allowing vertical brine movement throughout the sea-ice sheet. At this point, atmospheric CO₂ would have been available to the under-ice sea-water carbonate system, with ramifications for carbon cycling in sea-ice-dominated polar waters.

INTRODUCTION

Despite recent reductions in sea-ice concentration in the north polar seas (Maslanik and others, 2007; Comiso, 2008), ice cover remains a defining feature of the Northern Hemisphere, covering between approximately 6×10^6 and $15 \times 10^6\ \text{km}^2$ (US National Snow and Ice Data Center Sea Ice Index). Nonetheless, observations indicate that the cover is getting thinner (Rothrock and others, 2008; Kwok and others, 2009) and younger (Maslanik and others, 2007; Nghiem and others, 2007). Less is known about the role of sea ice on local, regional and global biogeochemical cycles relative to our understanding of the importance of sea ice to surface and atmospheric heat budgets (Serreze and Francis, 2006; Perovich and others, 2008). Most carbon-cycle research has not considered the possibility of either direct air–sea gas exchange in the presence of sea ice or indirect air–ice–sea gas exchange, where sea ice actively participates in CO₂ transfer. Therefore, global and regional budgets of air–sea CO₂ exchange have ignored ice-covered regions (Bates and Mathis, 2009, and references therein), relying instead on the assumption that a sea-ice cover is impermeable to gases. A growing body of recent research questions this assumption, as large fluxes of CO₂ have been reported over sea ice in winter (Miller and others, in press) and spring (Semiletov and others, 2004; Delille, 2006; Zemmelenk and others, 2006), while other work has highlighted a complex sea-ice carbonate system coupled to that of the upper mixed layer (Delille and others, 2007; Rysgaard and others, 2007, 2009; Miller and others, in press).

It is not unreasonable to expect sea ice to exchange CO₂ with the atmosphere given the rich biological communities in the ice (Thomas and Dieckmann, 2010) and the

temperature sensitivity of carbon speciation in both sea water (Zeebe and Wolf-Gladrow, 2001) and sea-ice brine (Papadimitriou and others, 2003). Ice algae can consume large quantities of carbon (Gosselin and others, 1997; Arrigo and others, 2010), and bacteria are so ubiquitous throughout the ice column that sea ice could even be net heterotrophic, despite photosynthetic CO₂ uptake at the bottom of the ice (Deming, 2010). Chemically, as sea water freezes, the increase in salinity of the resulting brine decreases gas solubility (Killawee and others, 1998; Mock and others, 2002; Tison and others, 2002) and this salting-out effect generally dominates over the decrease in temperature, which increases gas solubility. This net decrease in solubility as salinity increases and temperature decreases in ice brines appears to be true also of CO₂, despite complications associated with its aquatic acid-base chemistry. Calcium carbonate precipitation from the brines (Papadimitriou and others, 2003; Dieckmann and others, 2008, 2010) would also serve to increase pCO₂. Therefore, pCO₂ in sea-ice brines can be extremely high (Miller and others, in press) and, depending on the location within the sea-ice sheet, CO₂ can be exported either to the underlying sea water (Rysgaard and others, 2007; Miller and others, in press) or the overlying atmosphere (Nomura and others, 2006; Miller and others, in press).

Observations show that sea ice is depleted in both brine and CO₂ in late spring (Delille and others, 2007; Rysgaard and others, 2009), thereby encouraging CO₂ uptake. On warming, Tison and others (2008) reported evidence of convective overturning within Antarctic sea ice, whereby dense high-salinity brine was replaced by sea water. This process requires that sea ice be permeable to liquid

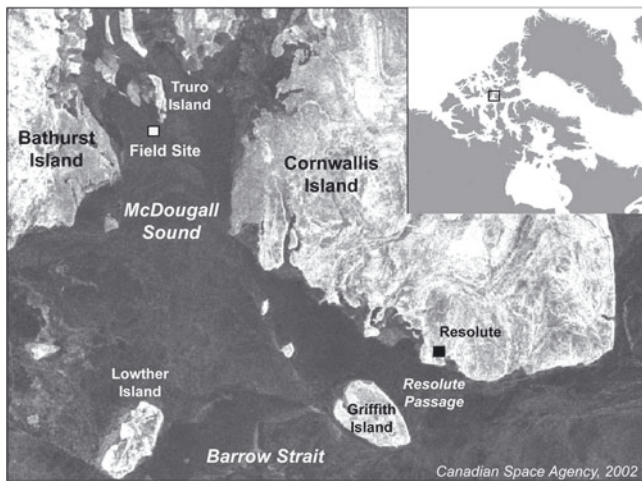


Fig. 1. Site location at 75.246° N, 97.283° W, near to the center of the Canadian Arctic Archipelago.

transport, which typically occurs at sea-ice brine volumes exceeding 5% (Golden and others, 1998) and provides a mechanism for replenishing sea-ice nutrients, including carbon. In addition, dissolution of any trapped CaCO₃ in the sea ice on warming would consume CO₂, decreasing pCO₂ and thereby encouraging an air-to-sea-ice CO₂ flux (Delille and others, 2007; Rysgaard and others, 2007).

The above-cited flux studies document exchanges that are episodic and potentially quite large and which seem to occur widely over sea ice in both hemispheres. Hence, it is important for CO₂ fluxes associated with sea ice to be considered in polar marine carbon-cycle studies (observations and modeling). Parameterizations are unlikely until the community is able to pinpoint the (seasonally varying) processes that control the exchanges. As yet, few measurements of CO₂ fluxes over sea ice exist, no doubt because the world's sea-ice cover constitutes a truly extreme environment, making field studies both expensive and logistically challenging. Further, equipment and sensors often are required to operate at the edge of their tolerances, making accurate measurements difficult. More case studies are required to consolidate our understanding of the relationships that exist between sea-ice CO₂ fluxes and the physical, chemical and biological components of the system.

In this paper we report the results of a study over seasonal sea ice during the spring of 2002 in the Canadian Arctic Archipelago (Fig. 1), where we measured heat, CO₂ and momentum fluxes in conjunction with measurements of the site's microclimate, including radiation balance and temperature structure. We have been able to identify relationships between the near-surface CO₂ flux and site energetics, but we are unable to relate the observed fluxes to changes in the ice cover's organic and inorganic carbon stores.

METHODS

The research site was situated over first-year sea ice in McDougall Sound approximately 3 km from the southwestern coast of Truro Island (75.2463° N, 97.2832° W) near the center of the Arctic Archipelago (Fig. 1). The flux station was situated on a pan of smooth landfast sea ice of uniform consolidation. Snow coverage on the pan varied from 5 to 50 cm, depending on the location of drifts. The ice

thickness around the site ranged from 1.45 to 1.50 m at the start of the experiment and increased to 1.57–1.60 m over the course of the experiment.

The air–surface CO₂ flux was measured between 9 May and 24 June 2002 using the eddy covariance technique. The flux system, a CSAT3 three-dimensional (3-D) ultrasonic anemometer (Campbell Scientific®, Logan, UT, USA) and LI-7500 open-path gas analyzer (LI-COR®, Lincoln, NE, USA), was mounted facing north at a height of 2.45 m above the snow surface. The gas analyzer was inclined at an angle of approximately 30°. Wind fetch (i.e. upstream distance of relatively uniform surface) from the measurement site exceeded 8 km across the angle arc between 300° and 60° from the flux system, as determined by a snowmobile survey and by positioning the site relative to land and adjacent floes on a synthetic aperture radar (SAR) image. Information on bulk meteorology, radiation fluxes, and snow and ice temperature was available from sensors mounted on and around this installation. Sensors were powered by a solar panel/battery array and periodically by a gas generator situated 250 m directly to the south of the instrument tower. Sensors were inspected daily to ensure that they remained in proper alignment and free of accumulated frost, snow or water. Turbulent fluctuations were scanned at 10 Hz using a data logger (model 23X, Campbell Scientific®, Logan, UT), while meteorological sensors, radiometers and thermocouple-based thermometers were scanned at 5 s intervals.

Trends in the turbulent fluctuations were removed through differencing, and the means, variances and covariances of the 3-D wind velocity, sonic temperature and scalar concentrations of CO₂ and H₂O were calculated through data-logger processing over 15 min periods. Post-processing of the data included a coordinate rotation of the covariances (McMillen, 1988) and density corrections for the CO₂ flux, including the Webb–Pearman–Leuning (WPL) correction (Webb and others, 1980) following Massman and Lee (2002), with an additional correction based on Burba and others (2008) to compensate for air density fluctuations in the gas analyzer's optical path associated with heating of the sensor. Sensor skin temperature required for the correction was estimated from air temperature using the multiple regression expression of Burba and others (2008) requiring both measured incident solar and long-wave radiation.

Data were screened on the basis of wind direction and periods unfavorable for flux measurements, including power interruptions, frost and rime occurrence, and excessively high and low winds. Favorable wind directions were northward of the angular arc between 300° and 60° to minimize possible impacts of both the tower and generator on measured wind and CO₂ concentration fluctuations. In addition, we noted that excessive tower vibration and blowing snow at wind speeds greater than approximately 12 m s⁻¹ resulted in excessively noisy flux measurements. Diagnostic information from the ultrasonic anemometer and gas analyzer provided an objective means of screening the data for periods of frost. Data were rejected if the diagnostic parameter for window purity (AGC) reported by the LI-7500 deviated from its clean window value. At low wind speed, turbulent mixing may be insufficient to extend the surface mixed layer to the height of the flux sensors. These data were removed using a cut-off based on a wind velocity of 2 m s⁻¹, which was determined graphically. Small gaps in the dataset (<3 h) were filled by linear interpolation. After screening, our

35 day flux record was distilled down to 18 days, leaving only those diurnal periods missing <3 hours of data.

Uncertainties in the eddy covariance estimates of the CO₂ flux have been discussed by Moncrieff and others (1996) and several others (including Goulden and others, 1996; Anthoni and others, 1999), and accuracy estimates range from $\pm 12\%$ to 25% of daytime values. The open-path eddy covariance system is well suited for remote deployment and has the advantage that the gas analyzer's optical path can be situated very close to the sonic anemometer. Although many studies have shown excellent agreement between open-path-derived CO₂ fluxes and those derived from other eddy covariance systems (Leuning and King, 1992; Hirata and others, 2007; Ibrom and others, 2007; Burba and others, 2008; Haslwanter and others, 2009; Järvi and others, 2009), other studies have shown that open-path systems can underestimate the CO₂ flux (i.e. underestimate efflux and overestimate uptake), thought to be associated with: (1) sensor heating during winter season applications (Burba and others, 2008; Lafleur and Humphries, 2008; Ono and others, 2008; Järvi and others, 2009); (2) lens contamination from dust and water during unattended deployments (Serrano-Orti and others, 2008); or (3) a cross-sensitivity between the open path's concentration measurements of CO₂ and H₂O in marine applications (Pyrtherch and others, 2010). Burba and others (2008) found that wintertime open-path CO₂ flux measurements were within $\pm 10\%$ of closed-path measurements over several ecosystems when the effect of instrument heating on the ambient flux is corrected using their empirical relationships, as we have done in this study. Ambient temperature ranged between -17.5°C and 0°C over our experiment, which is within the temperature range over which the correction of Burba and others (2008) was developed.

Sea-ice salinity and sea-water chemistry were available from water and ice samples extracted from a site approximately 4 km southwest of the flux tower. Ice cores for full salinity profiles were collected between 23 May (day of year (DOY) 143) and 3 June (DOY 156) (Johnston, 2006). The ice brine volume and salinity were estimated using the expressions of Cox and Weeks (1983) and measured sea-ice bulk density, salinity and temperature profiles (details appear in Mundy, 2003). Chlorophyll *a* (Chl *a*) accumulation within the bottom 5 cm of the sea ice was also measured three to four times a week (Mundy and others, 2005).

Surface sea water was sampled through a hole in the sea ice from 1 May to 9 June and water samples were analyzed for total inorganic carbon (TIC), total alkalinity (A_T), salinity and temperature. Sea water was extracted at 0.5 m depth below the ice base using GoFlo bottles prior to 7 May and using a subpump (e.g. Pondmaster Supreme Mag Drive) thereafter (Miller and others, in press). The samples were collected into triplicate 250 mL glass bottles and poisoned with 100 μL of saturated HgCl₂ solution. The ground glass stoppers were sealed with grease and elastic closures and the samples were stored cold, but not frozen, until analysis at the Institute of Ocean Sciences (Sidney, British Columbia, Canada) within 4 months (Dickson and Goyet, 1994). Temperature was determined using a hand-held temperature probe placed in the outflow from the pump.

The TIC analyses were conducted by colometric titration with a SOMMA extraction system (Johnson and others, 1993), while alkalinity was determined by potentiometric titration using an open cell with end-point determination using the modified Gran plot (Hansson and Jagner, 1973;

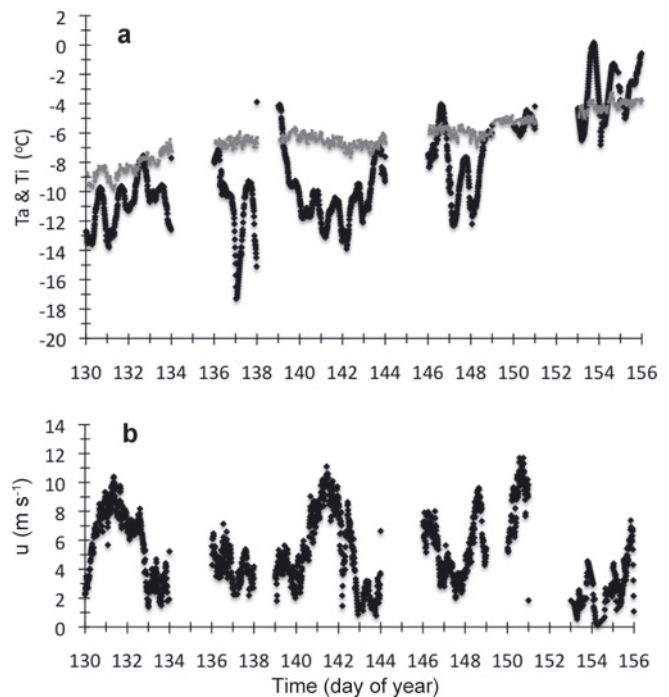


Fig. 2. Time series of temperature and wind speed at the sampling site. (a) Hourly temperatures: air (T_a) in black; snow–ice interface (T_i) in grey. (b) Hourly wind speed (u).

Haraldsson and others, 1997). Both sets of analyses were calibrated using certified reference materials provided by A. Dickson of Scripps Institution of Oceanography, USA, and precision, based on the standard deviations between triplicate samples, was $2 \mu\text{mol kg}^{-1}$ for both TIC and A_T . Salinity was measured on the remains of the TIC/ A_T samples at the end of November 2002 using a Guildline Portasal model 8410 salinometer and calibrated with IAPSO (International Association of Meteorology and Atmospheric Sciences) standard sea water. We estimate that the error in salinity associated with the added mercuric chloride is <0.03 (psu).

RESULTS AND DISCUSSION

Environmental physical and chemical context

The 26 day experiment encompassed the period of transition from an early spring cold snowpack through to a period of snowmelt and melt-pond formation. Air temperature was highly variable throughout the study (Fig. 2), and the first positive air temperature was recorded on 2 June (DOY 153). The temperature at the ice–snow interface ranged from -9.8°C at the onset of the experiment to a maximum value of -3.2°C near the end of the experiment. The ice surface warmed rapidly between 10 and 19 May (DOY 130–139) and after 26 May (DOY 148). Storms centered on 11 May (DOY 131), 21 May (DOY 141) and 25–30 May (DOY 145–150) were associated with high surface winds. Gaps in the time series correspond to periods of particularly harsh weather, including blizzard and/or ice-riming conditions.

The ice surface and snow-base environments were both saline (Fig. 3a). Upwardly decreasing salinity gradients in snow over seasonal sea ice are common (e.g. Barber and others, 1995; Langlois and others, 2007). Salinity at the ice surface and 2 cm into the snowpack varied between 5.9 and

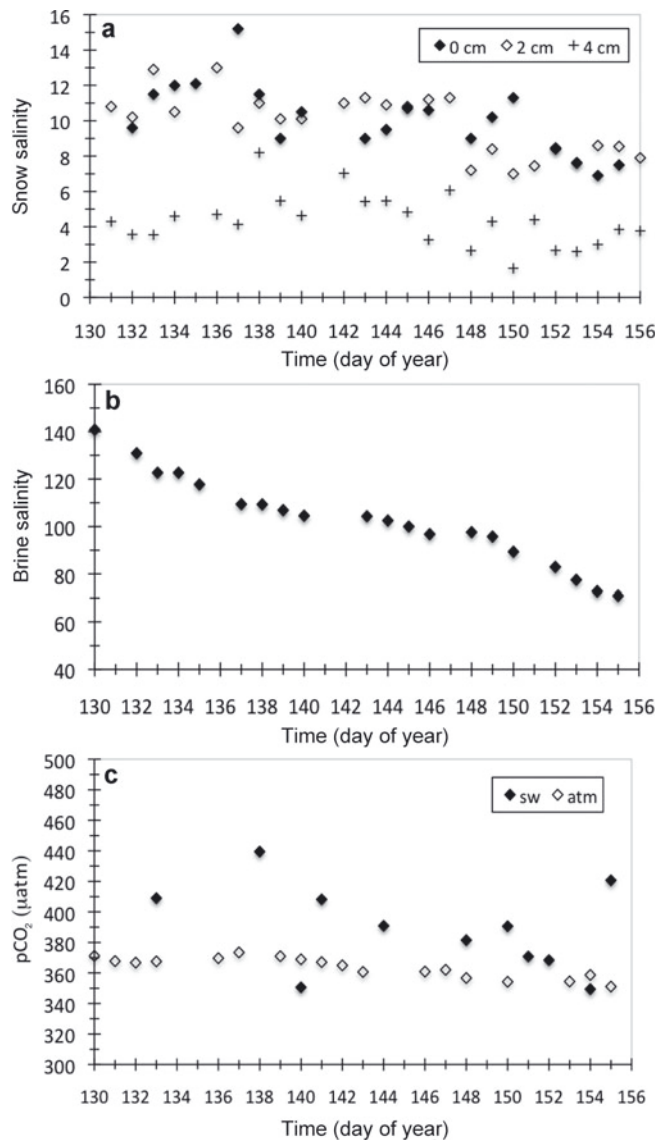


Fig. 3. Time series of: (a) salinity at the snow base (ice surface) and 2 and 4 cm up into the snowpack; (b) brine salinity for temperatures measured at the snow–ice interface; (c) pCO₂ in the air (open diamond) and in surface sea water (0.5 m under the sea ice; solid diamond).

15.3 over our experiment and decreased sharply with distance away from the snow base. At 4 cm from the snow base, the salinity was on average 3.5 less than at the snow–ice interface, while at 6 cm from the snow base the salinity ranged from 0 to 3 (not shown). Snow salinity decreased significantly after 25 May (DOY 145) at 4 cm up from the snow base and 30 May (DOY 150) at the ice surface, presumably the result of snowmelt. Ice salinity profiles showed a weak ‘C-shape’ distribution (not shown), averaging 7.5 ± 0.8 in the upper 15 cm of the cores and 5.1 ± 0.6 between 30 and 120 cm. The brine salinity at the ice surface (calculated from measured temperatures) decreased over the experiment from 140 to 70 (Fig. 3b) as a result of dilution by melting. Surface sea-water salinity below the ice fluctuated between 32.65 and 32.74, with no obvious trend (not shown). Sea-water pCO₂ (as calculated from TIC and A_T) declined over the period 18 May–4 June (DOY 138–155), yet remained supersaturated relative to atmospheric levels until late in the experiment (Fig. 3c).

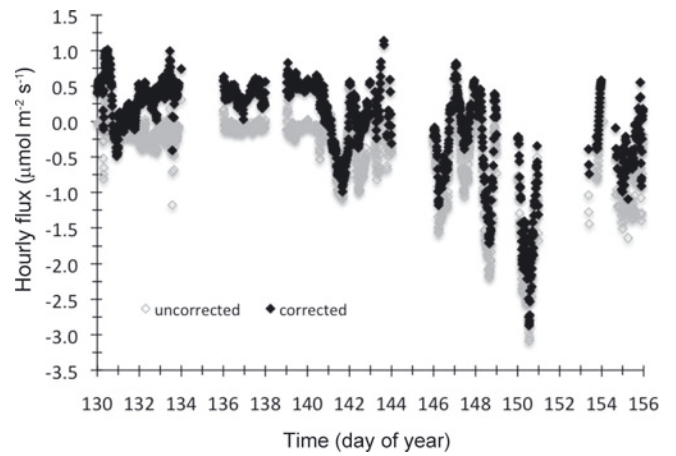


Fig. 4. Running mean (5 hour window) of hourly CO₂ flux (FCO₂). Fluxes corrected for sensor heating are shown in black, while uncorrected fluxes appear as grey. A negative flux is directed downwards, toward the snow surface.

Springtime air–surface CO₂ exchange

Figure 4 shows the hourly and daily average air–surface CO₂ exchange. The corrected flux tended to show a low-level CO₂ efflux (averaging $0.36 \mu\text{mol m}^{-2} \text{s}^{-1}$) prior to 20 May (DOY 140), followed by periods of moderate to strong CO₂ uptake. Maximum hourly efflux exceeded $1.0 \mu\text{mol m}^{-2} \text{s}^{-1}$, while hourly uptake approached $-3.0 \mu\text{mol m}^{-2} \text{s}^{-1}$ on 30 May (DOY 150).

The maximum uptake rates in Figure 4 are in excess of any other values reported over sea ice to date (Semiletov and others, 2004; Zemmeling and others, 2006; Miller and others, in press) and are two to four times larger than hourly fluxes observed over the North Atlantic (McGillis and others, 2001). The fluxes observed by Semiletov and others (2004) approached $-0.8 \mu\text{mol m}^{-2} \text{s}^{-1}$ over first-year sea ice near Barrow, Alaska, while Zemmeling and others (2006) reported fluxes up to $-0.3 \mu\text{mol m}^{-2} \text{s}^{-1}$ over ablating Antarctic multi-year ice. In both of these studies, the CO₂ fluxes were measured using eddy covariance systems with open-path CO₂ sensors, consistent with this study, but without the correction of Burba and others (2008). Wintertime CO₂ fluxes reported by Miller and others (in press) over fast ice in the western Canadian Arctic showed considerable variability and were also during isolated periods quite large. The fluxes were generally directed upward (median flux of $0.14 \mu\text{mol m}^{-2} \text{s}^{-1}$). In that work, we speculated that the exchange was driven by some combination of sea-ice brine carbonate chemistry and biological activity. By comparison, wintertime hourly efflux in cold terrestrial systems can range anywhere between $0.25 \mu\text{mol m}^{-2} \text{s}^{-1}$ for wetlands (e.g. Lafleur and others, 2003) and approximately $0.45 \mu\text{mol m}^{-2} \text{s}^{-1}$ for upland boreal forest soils in Alaska (Sullivan and others, 2008).

Fick’s law for gas diffusion dictates that we would require a CO₂ concentration at the snow base of approximately 38 mmol m^{-3} , roughly twice atmospheric levels, to sustain our average early experiment diffusive CO₂ efflux ($0.36 \mu\text{mol m}^{-2} \text{s}^{-1}$) through the snow, assuming a snow depth of 0.3 m and diffusivity of $0.05 \text{ cm}^2 \text{ s}^{-1}$. Diffusivity for gas transport in wind-packed snow can range between 0.02 and $0.08 \text{ cm}^2 \text{ s}^{-1}$ (Albert and Shultze, 2002). An upward flux of $0.36 \mu\text{mol m}^{-2} \text{s}^{-1}$ is not inconsistent with

field observations elsewhere, which indicate that sea-ice pCO₂ in the spring can exceed atmospheric values (Delille and others, 2007) and perhaps significantly so (Miller and others, in press). In laboratory experiments, Nomura and others, (2006) observed low-level CO₂ efflux from growing sea ice at a rate (0.004–0.012 μmol CO₂ m⁻² s⁻¹) that increased with increasing brine salinity (decreasing brine temperature). Ice temperature in their experiments ranged between –2.7°C and –4.1°C, which is warmer than our near-surface sea ice for all but the final days of our experiment (Fig. 2). Consequently, brine salinity in their study was lower by almost a factor of 2, which could partly explain why our observed average efflux was higher.

As the under-ice sea water was supersaturated in pCO₂ relative to atmospheric values for most of our study (Fig. 3c), the prevailing ocean–air pCO₂ gradient could also support an upward flux of CO₂. Through much of the study, the ice in McDougall Sound was likely impermeable to brine because the brine volume constituted <5% (the cut-off for brine permeability in columnar sea ice; Golden and others, 1998) of the sea-ice interior prior to 26 May (DOY 146) (Fig. 5) and hence CO₂ probably could not have been transported by the brine. However, little is known about the comparable temperature cut-off for gas diffusion in sea ice, aside from the laboratory study of Gosink and others (1976) who observed substantial transport of halogenated gases at temperatures down to –15°C. The results from Gosink and others (1976) imply that CO₂ could have been moving through the ice throughout our study, something that we cannot confirm.

Spring heating raised the ice temperature above –5°C by 28 May (DOY 148), with a corresponding increase in sea-ice brine volume above 5% (Fig. 5). Beyond this date, the brine should have been draining freely and mixing with the underlying sea water (Golden and others, 1998; Tison and others, 2008). The timing of this transition closely corresponded to the period of maximum CO₂ uptake observed between 28 and 30 May (DOY 148–150; Fig. 4), meaning that atmospheric CO₂ could have offset part of any pCO₂ deficit developing at the ice–water interface as a result of algal production or melt dilution. In regard to the former, sea ice in the Canadian Arctic Archipelago ranks amongst the most productive in the Arctic, with reported primary production rates between 20 and 463 mg C m⁻² d⁻¹ (Arrigo and others, 2010). Chl *a* concentrations within the bottom 5 cm of the ice cover close to our research site (Mundy and others, 2005) were between 20 and 45 mg m⁻² by 29 May (DOY 149). Data shown by Lavoie and others (2005) indicate that pronounced ice algal accumulation in 2002 (commensurate with our study) had started at about 10 May (DOY 130) and persisted into the first week of June (approximately DOY 160) in sea ice approximately 70 km southeast of our study site and of comparable thickness and snow depth. Maximum Chl *a* concentration ranged between 55 and 80 mg m⁻² at their site, with net particulate organic carbon (POC) accumulation rates ranging between 28 and 55 mg C m⁻² d⁻¹, depending on snow thickness. Algae are the main contributors of POC at the base of Arctic first-year sea ice (Riedel and others, 2008). Accumulation rates were obtained by applying a POC:Chl *a* ratio of 20 (Riedel and others, 2008) to Chl *a* time rate-of-change estimates obtained graphically from figures provided by Lavoie and others (2005), over the period between 10 May (DOY 130) and 25 May or 10 June (DOY 145 or 161) for thick and thin snow, respectively. Uptake, according to our tower measurements, averaged

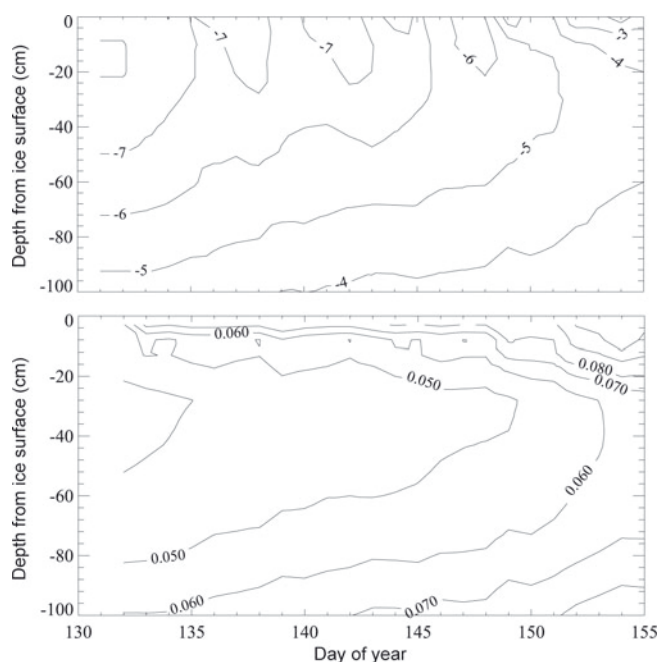


Fig. 5. The evolution of the 1200 h (local time: North American Central Standard Time) temperature and brine volumetric fraction in the upper meter of sea ice.

approximately 23 mg C m⁻² d⁻¹ between 10 and 30 May (DOY 130–150). This value is close in magnitude to the POC accumulation rates that we derived from Lavoie and others (2005) and on the low end of primary production rates reported for sea ice in the Canadian Arctic Archipelago. Although we expect the ocean mixed layer to be the main supplier of nutrients to the skeletal layer at the ice base (Thomas and others, 2010, and references therein), it is not inconceivable for atmospheric CO₂, via brine drainage, to offset short-term CO₂ deficits at the ice base given that: (1) both TIC and CO₂(aq) in sea-ice brine can be depleted under conditions of high primary production and large accumulation of algal biomass (Thomas and others, 2010, and references therein); (2) the nutrient supply from the mixed layer to biomass at the ice base can be restricted by the thickness of the molecular sublayer (Lavoie and others, 2005); and (3) downward flushing of nutrients into sea ice associated with snowmelt has been documented and thought able to augment sea-ice biomass accumulation (e.g. Granskog and others, 2003).

Finally, if CaCO₃ had precipitated in the ice when it formed, the late-spring melting process would have dissolved the salts, lowering pCO₂ within the ice and further encouraging CO₂ drawdown from the atmosphere. Collectively, these observations support the argument that the observed late-season CO₂ uptake was a result of a permeable ice cover and a lowering of pCO₂ in the ice and sea water through photosynthesis, melt and possibly calcium carbonate dissolution.

The magnitude of fluxes reported here raises concerns about possible measurement biases associated with the open-path system. It is evident (Fig. 4) that prior to 20 May (DOY 140) the heating correction constituted a large component of the corrected flux, often changing the flux direction from predominately a regime of low-level uptake to low-level efflux. Accordingly, we are less confident of measurements during this period given the possibility that

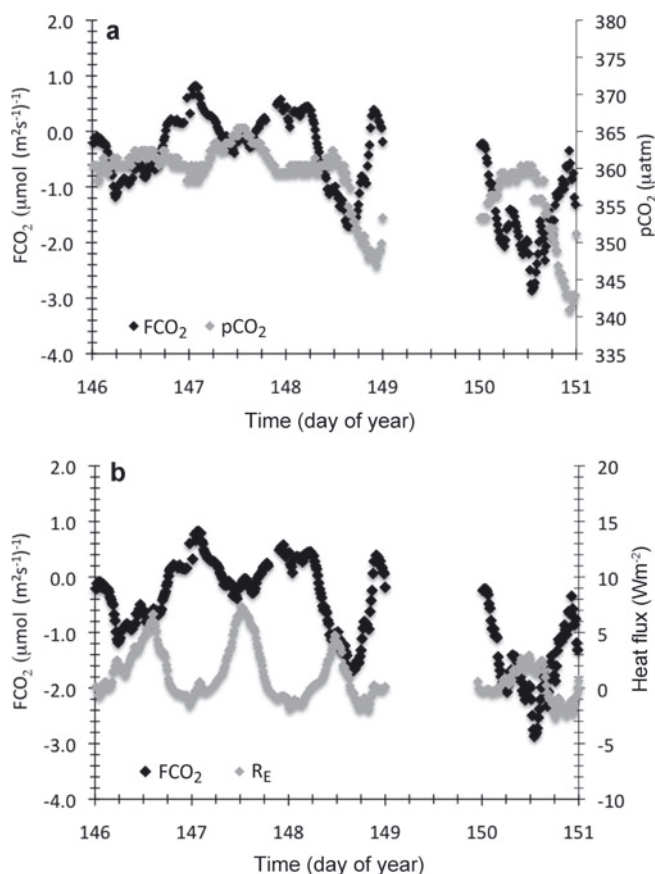


Fig. 6. The time series of average (a) atmospheric pCO₂ and (b) latent heat flux (R_E) between 26 and 31 May (DOY 146–151). The flux of CO₂ (FCO_2) is provided in both plots for reference.

the flux has been overcorrected (Järvi and others, 2009) and hence is artificially high. With this uncertainty a validation of the open-path eddy covariance system, and associated corrections, is required over sea ice to confirm that low-level fluxes of this sort are in fact above system noise. However, the heating correction to the CO₂ flux represents only a small component of the strong midday uptake that occurred on 21, 28 and 30 May and 3 June (DOY 141, 148, 150 and 154). We are also reasonably confident that the measured uptake at these times is not the result of an obstruction of the open-path lens (Serrano-Orti and others, 2008) or cross-sensitivity to the water vapour flux (Pyrtherch and others, 2010). In regard to the former, we do observe a decrease in atmospheric CO₂ concentration of 4–5% corresponding to CO₂ uptake on 28 and 30 May (DOY 148 and 150) (Fig. 6a), which if related to lens obstruction would artificially lower our flux measurement by as much as 30% through a reduction in the WPL correction (Serrano-Orti and others 2008). The sensor lens was checked for cleanliness daily, and diurnal fluctuations in ambient CO₂ of >10% are not uncommon over ecosystems with strong 24 hour cycles of net photosynthesis (Anthoni and others, 1999; Yang and others, 1999), hence we expect our measurements over these periods to be within the sensor's specifications. High-frequency measurements of CO₂ and H₂O concentration are not available from this study to explore possible sensor cross-sensitivity, but data from subsequent experiments over winter- or springtime sea ice show no coherent relationship between high-frequency measurements of CO₂ mixing ratio

and relative humidity. Further, our measured latent heat flux ($\pm 7 \text{ W m}^{-2}$) between 26 and 31 May (DOY 146–151; Fig. 6b) is close to a factor of 10 smaller than reported in Pyrtherch and others (2010) over open water, indicating that if there was cross-sensitivity in the gas concentration measurements, it was not strongly correlated to vertical velocity or, hence, the CO₂ flux.

Diurnal variation in air–surface CO₂ exchange

Prominent shifts from efflux to uptake were observed several times, including on 10 May (DOY 130), 21–22 May (DOY 141–142) and then 26, 28 and 30 May and 2 June (DOY 146, 148, 150 and 155) (Fig. 4). Two periods with large CO₂ flux (FCO_2) ranges are shown in Figure 7a, showing the measured flux between 20 and 24 May (DOY 140–142) and between 26 and 30 May (DOY 146–150). Also shown are the corresponding variations in surface net radiation (R_n , Fig. 7b), ice surface temperature (T_i , Fig. 7c), horizontal wind speed (u , Fig. 7d) and air temperature (T_a , Fig. 7e). The interface temperature reflects the thermodynamic state of the surface. Net radiation provides a measure of heating and cooling of the surface via radiation, while horizontal wind speed is related to surface shear and forced convection.

Uptake on 21 May (DOY 141) started during the night of 20 May (DOY 140) and increased over the course of the morning and afternoon of 21 May (Fig. 7a). The uptake occurred during the first high wind event following the intense heating of the snowpack on 19 May (DOY 139) (Fig. 2). The start of the CO₂ uptake during the evening of 20 May (DOY 140) coincided with the rise in wind speed (Fig. 7d), and uptake stopped when the wind speed dropped again below 6 m s^{-1} in the early morning of 22 May (DOY 142). The Gaussian-shaped timeline of hourly R_n centered midday on 21 May (DOY 141; Fig. 7b) indicates clear-sky conditions, which allowed the surface to cool intensely over much of the night. Peak uptake on 21 May (DOY 141) also corresponded in time to the 24 hour maximum in R_n and a rise in T_i . The efflux observed at about midnight at the start of 22 May (DOY 142) corresponded to the 24 hour minimum in R_n .

Strong CO₂ uptake was also observed on 26, 28 and 30 May (DOY 146, 148 and 150), with efflux occurring just about midnight on 27 and 28 May (DOY 147 and 148). The periods of efflux corresponded to night-time minima in R_n , air temperature and cooling at the snow base, again associated with clear-sky conditions. Over this period, the hourly pattern in FCO_2 mirrored wind speed. High winds (generally $>6 \text{ m s}^{-1}$) gave rise to large CO₂ uptake rates, and low winds corresponded to periods of little exchange or efflux. The largest uptake rate observed over the entire experiment occurred on 30 May (DOY 150) under conditions of extremely high wind speed ($>9 \text{ m s}^{-1}$) and high interface (greater than -5.5°C) and air (approximately -5°C) temperatures.

We conclude that, in general, CO₂ uptake and efflux mirrored wind speed, with winds in excess of approximately $5\text{--}6 \text{ m s}^{-1}$ supporting uptake, while lighter winds were associated with efflux. The relationship between wind speed and FCO_2 is nonlinear in nature, as evident in Figure 8 for the period 26–30 May (DOY 146–150). High winds ventilate the snow (Colbeck, 1989; Albert and Shultz, 2002) and above a variable threshold ($4.4\text{--}11.0 \text{ m s}^{-1}$) give rise to blowing snow (Li and Pomeroy, 1997). Snow ventilation allows exchange between the atmosphere and saline snow

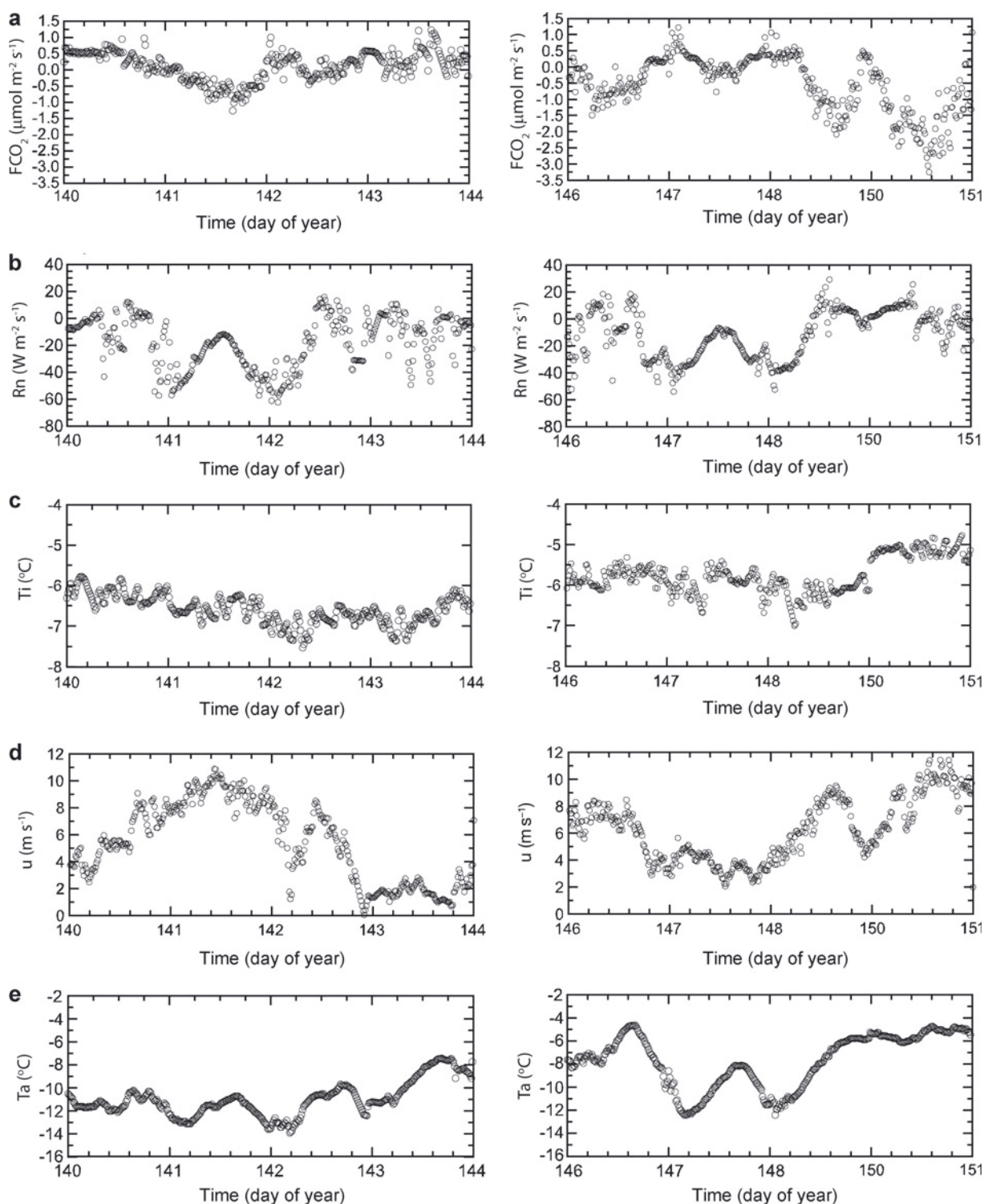


Fig. 7. Hourly variation in (a) CO₂ flux (FCO_2), (b) surface net radiation (R_n), (c) snow-ice interface temperature (T_i), (d) wind speed (u) and (e) air temperature (T_a) for the periods 20–23 May (DOY 140–143) and 26–30 May (DOY 146–150). No data are available from 29 May (DOY 149).

base/ice surface. In addition, blowing snow has a high surface area:mass ratio and is subject to intense atmospheric turbulence, hence the potential for turbulent transfer of trace gases (in addition to heat) to and from the snow grains (Pomeroy and others, 1999) or, in our case, brine-wetted snow grains. The efficiency of gas adsorption/desorption on ice grains will be proportional to the changing snow surface area (Legagneux and others, 2002). Hence, blowing snow during conditions conducive to down-directed sensible

heating (i.e. a warming atmosphere) allows for rapid heating of the brine-wetted snow base and ice surface by convection in the snow. On the other hand, in the absence of high winds, CO₂ exchange with the snow base and ice surface is controlled by diffusion, and the upper snow may moderate the exchange by storing air (and CO₂).

Uptake also corresponded to local peaks in both net radiation and temperature, while efflux generally occurred in association with local minima in net radiation and

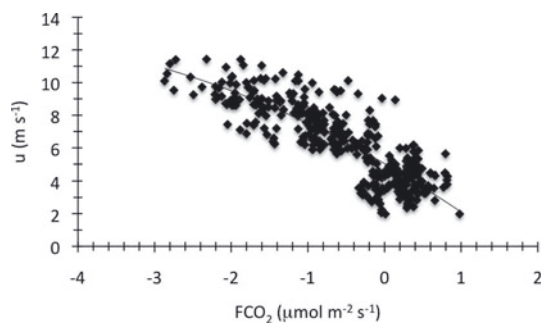


Fig. 8. Relationships between the measured CO₂ flux and wind speed between 26 and 30 May (DOY 146–150). The trend line fit to the data is a second-order polynomial.

temperature, which occurred largely at night. Previous studies have shown that the dielectric properties of brine-wetted snow and sea ice are quite sensitive to incident radiation (long- and shortwave) through changing brine volume at the snow base (Barber and others, 1995; Barber and Thomas, 1998; Langlois and others, 2008). Reduced radiative cooling (increased net radiation) allows the snow/ice system to retain a greater proportion of energy available from both oceanic and atmospheric sensible heat, thereby supporting warming. The opposite occurs during periods of pronounced radiation loss.

Our data indicate that the diurnal fluctuations in meteorological conditions can largely explain the efflux and uptake sequences we observed. Nocturnal cooling and freezing of the brine at the snow base and ice surface degasses CO₂ through a reduced solubility in the brine (Killawee and others, 1998; Mock and others, 2002; Tison and others, 2002) and possibly precipitation of calcium carbonate (Papadimitriou and others, 2003). It follows that the midday uptake often observed with warming was associated with any combination of: increasing gas solubility in the brines in the upper sea ice and snow base; strong air-to-brine pCO₂ gradients associated with nocturnal degassing and CO₂ depletion in the brine (Delille and others, 2007; Rysgaard and others, 2007); and possibly dissolution of calcium carbonate (Papadimitriou and others, 2003). The pattern of daytime uptake and nocturnal efflux observed here is indicative of a biologically controlled system of diurnal photosynthesis and respiration. Although we are unable to explore relationships to biology with this dataset, it is intuitive that net photosynthesis could contribute to our observed daytime CO₂ uptake, given the dependency of photosynthesis on photosynthetically active radiation.

SUMMARY AND CONCLUSIONS

We measured springtime CO₂ fluxes over seasonal sea ice in the Canadian Arctic Archipelago that were much greater than reported observations from other studies over sea ice (Semiletov and others, 2004; Zemmeling and others, 2006; Miller and others, in press). Efflux tended to dominate the exchange early in the experiment, when sea-ice surface temperature was less than approximately -6°C , giving rise to episodes of increasingly large rates of uptake as the sea ice warmed.

Diurnal variation of the CO₂ flux (both the direction and magnitude) corresponded to fluctuations in basic micro-meteorological variables. Uptake of CO₂ was generally

associated with warming in the presence of high winds, while cooling and low winds gave rise to CO₂ effluxes. In general, uptake rarely occurred when the wind speed was $<4.5\text{ m s}^{-1}$. The high wind speeds associated with uptake ($>6\text{ m s}^{-1}$) suggest that ventilation of, and turbulent exchange with, the snow are an important part of the process. The flux may also be influenced by calcium carbonate precipitation and dissolution at the brine-wetted snow base and upper sea-ice surface.

Early in the season (ice temperature less than -6°C), the sea ice appears to be a source of atmospheric CO₂, consistent with observations from a winter study (Miller and others, in press), also over seasonal sea ice. Later in the season, the magnitude of uptake increases as the ice surface temperature increases past -5°C , corresponding to an increase in brine volume and permeability, permitting vertical drainage and coupling with the underlying sea water.

These findings raise the prospect of atmospheric CO₂ directly contributing to the sea-water carbon drawdown in the presence of an ice cover, with consequences for both basic carbon budgets and biophysical modeling of ice ecosystem environments. Further CO₂ flux studies over sea ice, particularly those involving the simultaneous deployment of open- and closed-path eddy covariance systems in conjunction with measurements of time-dependent sea-ice carbon inventory, are required to confirm the robustness of existing corrections to eddy covariance CO₂ flux measurements and the spatial relevance of the processes described here.

ACKNOWLEDGEMENTS

Sea-ice camps are inherently expensive to operate and numerous investigators and agencies participated in the C-ICE 2002 experiment. This research was largely funded by a Natural Sciences and Engineering Research Council of Canada (NSERC) grant (Discovery) to T. Papakyriakou and the Department of Fisheries and Oceans Canada (DFO) Strategic Science Fund (L. Miller). Resources for infrastructure and logistics were shared among several agencies, including Natural Resources Canada, Environment Canada (Canadian Ice Service), NSERC and the University of Manitoba (Centre for Earth Observation Science). We thank D. Arychuk, M. Davelaar, M. Fortier, K. Johnston, C.J. Mundy, K. Morris and O. Owens for field and laboratory assistance, and the reviewers and the scientific editor for their valuable suggestions. We thank the Polar Continental Shelf Project (PCSP) for logistical support.

REFERENCES

- Albert, M.R. and E. Shultz. 2002. Snow and firn properties and air-snow transport processes at Summit, Greenland. *Atmos. Environ.*, **36**(15–16), 2789–2797.
- Anthoni, P.M., B.E. Law and M.H. Unsworth. 1999. Carbon and water vapor exchange of an open-canopied ponderosa pine ecosystem. *Agric. Forest Meteorol.*, **95**(3), 151–168.
- Arrigo, K.R., T. Mock and M.P. Lizotte. 2010. Primary producers and sea ice. In Thomas, D.N. and G.S. Dieckmann, eds. *Sea ice, Second Edition*. Chichester, Wiley-Blackwell, 283–326.
- Barber, D.G. and A. Thomas. 1998. The influence of cloud cover on the radiation budget, physical properties, and microwave scattering coefficient (σ^0). *IEEE Trans. Geosci. Remote Sens.*, **36**(1), 38–50.
- Barber, D.G., T.N. Papakyriakou, E.F. LeDrew and M.E. Shokr. 1995. An examination of the relation between the spring period

- evolution of the scattering coefficient (σ^0) and radiative fluxes over landfast sea-ice. *Int. J. Remote Sens.*, **16**(17), 3343–3363.
- Bates, N.R. and J.T. Mathis. 2009. The Arctic Ocean marine carbon cycle: evaluation of air–sea CO₂ exchanges, ocean acidification impacts and potential feedbacks. *Biogeosciences*, **6**(11), 2433–2459.
- Burba, G.G., D.K. McDermitt, A. Grelle, D.J. Anderson and L. Xu. 2008. Addressing the influence of instrument surface heat exchange on the measurements of CO₂ flux from open-path gas analyzers. *Global Change Biol.*, **14**(8), 1854–1876.
- Colbeck, S.C. 1989. Air movement in snow due to windpumping. *J. Glaciol.*, **35**(120), 209–213.
- Comiso, J.C. 2008. Trends in the sea ice cover using enhanced and compatible AMSR-E, SSM/I, and SMMR data. *J. Geophys. Res.*, **113**(C2), C02S07. (10.1029/2007JC004257.)
- Cox, G.F.N. and W.F. Weeks. 1983. Equations for determining the gas and brine volumes in sea-ice samples. *J. Glaciol.*, **29**(102), 306–316.
- Delille, B. 2006. Inorganic carbon dynamics and air–ice–sea CO₂ fluxes in the open and coastal waters of the Southern Ocean. (PhD thesis, University of Liège.)
- Delille, B., B. Jourdain, A.V. Borges, J.-L. Tison and D. Delille. 2007. Biogas (CO₂, O₂, dimethylsulfide) dynamics in spring Antarctic fast ice. *Limnol. Oceanogr.*, **52**(4), 1367–1379.
- Deming, J.W. 2010. Sea ice bacteria and viruses. In Thomas, D.N. and G.S. Dieckmann, eds. *Sea ice. Second edition*. Chichester, Wiley-Blackwell, 247–282.
- Dickson, A.G. and C. Goyet, eds. 1994. *Handbook of methods for the analysis of the various parameters of the carbon dioxide system in sea water, version 2.0*. Oak Ridge, TN, US Department of Energy. Oak Ridge National Laboratory. (ORNL/CDIAC-74.)
- Dieckmann, G.S. and 7 others. 2008. Calcium carbonate as ikaite crystals in Antarctic sea ice. *Geophys. Res. Lett.*, **35**(8), L08501. (10.1029/2008GL033540.)
- Dieckmann, G.S. and 6 others. 2010. Brief communication: ikaite (CaCO₃•6H₂O) discovered in Arctic sea ice. *Cryos. Discuss.*, **4**(1), 153–161.
- Golden, K.M., S.F. Ackley and V.I. Lytle. 1998. The percolation phase transition in sea ice. *Science*, **282**(5397), 2238–2241.
- Gosink, T.A., J.G. Pearson and J.J. Kelley. 1976. Gas movement through sea ice. *Nature*, **263**(5572), 41–42.
- Gosselin, M., M. Leveseur, P.A. Wheeler, R.A. Horner and B.C. Booth. 1997. New measurements of phytoplankton and ice algal production in the Arctic Ocean. *Deep-Sea Res. II*, **44**(8), 1623–1625.
- Goulden, M.L., J.W. Munger, S.-M. Fan, B.C. Daube and S.C. Wofsy. 1996. Measurements of carbon sequestration by long-term eddy covariance: methods and a critical evaluation of accuracy. *Global Change Biol.*, **2**(3), 169–182.
- Granskog, M.A., H. Kaartokallio and K. Shirasawa. 2003. Nutrient status of Baltic Sea ice – evidence for control by snow-ice formation, ice permeability, and ice algae. *J. Geophys. Res.*, **108**(C8), 3253. (10.1029/2002JC001386.)
- Hansson, I. and D. Jagner. 1973. Evaluation of the accuracy of gran plots by means of computer calculations: application to the potentiometric titration of the total alkalinity and carbonate content in sea water. *Anal. Chim. Acta*, **65**(2), 363–373.
- Haraldsson, C., L.G. Anderson, M. Hassellöv, S. Hulth and K. Olsson. 1997. Rapid, high-precision potentiometric titration of alkalinity in ocean and sediment pore waters. *Deep-Sea Res. I*, **44**(12), 2031–2044.
- Haslwanter, A., A. Hammerle and G. Wohlfahrt. 2009. Open-path vs. closed-path eddy covariance measurements of the net ecosystem carbon dioxide and water vapour exchange: a long-term perspective. *Agric. Forest Meteorol.*, **149**(2), 291–302.
- Hirata, R. and 7 others. 2007. Seasonal and interannual variations in carbon dioxide exchange of a temperate larch forest. *Agric. Forest Meteorol.*, **147**(3–4), 110–124.
- Ibrom, A., E. Dellwik, S.E. Larsen and K. Pilegaard. 2007. On the use of the Webb–Pearman–Leuning theory for closed-path eddy correlation measurements. *Tellus A*, **59**(5), 937–946.
- Järvi, L. and 8 others. 2009. Comparison of net CO₂ fluxes measured with open- and closed-path infrared gas analyzers in an urban complex environment. *Boreal Environ. Res.*, **14**(4), 499–514.
- Johnson, K.M., K.D. Wills, D.B. Butler, W.K. Johnson and C.S. Wong. 1993. Coulometric total carbon dioxide analysis for marine studies: maximizing the performance of an automated gas extraction system and coulometric detector. *Mar. Chem.*, **44**(2–4), 167–187.
- Johnston, M. 2006. A comparison of physical properties and strength of decaying first-year ice in the Arctic and sub-Arctic. *Ann. Glaciol.*, **44**, 154–162.
- Killawee, J.A., I.J. Fairchild, J.L. Tison, L. Janssens and R. Lorrain. 1998. Segregation of solutes and gases in experimental freezing of dilute solutions: implications for natural glacial systems. *Geochim. Cosmochim. Acta*, **62**(23–24), 3637–3655.
- Kwok, R., G.F. Cunningham, M. Wensnahan, I. Rigor, H.J. Zwally and D. Yi. 2009. Thinning and volume loss of the Arctic Ocean sea ice cover: 2003–2008. *J. Geophys. Res.*, **114**(C7), C07005. (10.1029/2009JC005312.)
- Lafleur, P.M. and E.R. Humphreys. 2008. Spring warming and carbon dioxide exchange over low Arctic tundra in central Canada. *Global Change Biol.*, **14**(4), 740–756.
- Lafleur, P.M., N.T. Routet, J.L. Bubier, S. Frolking and T.R. Moore. 2003. Interannual variability in the peatland–atmosphere carbon dioxide exchange at an ombrotrophic bog. *Global Biogeochem. Cycles*, **17**(2), 1036. (10.1029/2002GB001983.)
- Langlois, A., C.J. Mundy and D.G. Barber. 2007. On the winter evolution of snow thermophysical properties over land-fast first-year sea ice. *Hydrol. Process.*, **21**(6), 705–716.
- Langlois, A., T. Fisco, D.G. Barber and T.N. Papakyriakou. 2008. Response of snow thermophysical processes to the passage of a polar low-pressure system and its impact on in situ passive microwave radiometry: a case study. *J. Geophys. Res.*, **113**(C3), C03S04. (10.1029/2007JC004197.)
- Lavoie, D., K. Denman and C. Michel. 2005. Modeling ice algal growth and decline in a seasonally ice-covered region of the Arctic (Resolute Passage, Canadian Archipelago). *J. Geophys. Res.*, **110**(C11), C11009. (10.1029/2005JC002922.)
- Legagneux, L., A. Cabanes and F. Dominé. 2002. Measurement of the specific surface area of 176 snow samples using methane adsorption at 77 K. *J. Geophys. Res.*, **107**(D17), 4335. (10.1029/2001JD001016.)
- Leuning, R. and K.M. King. 1992. Comparison of eddy-covariance measurements of CO₂ fluxes by open- and closed-path CO₂ analysers. *Bound.-Layer Meteorol.*, **59**(3), 297–311.
- Li, L. and J.W. Pomeroy. 1997. Estimates of threshold wind speeds for snow transport using meteorological data. *J. Appl. Meteorol.*, **36**(3), 205–213.
- McGillis, W.R., J.B. Edson, J.E. Hare and C.W. Fairall. 2001. Direct covariance air–sea CO₂ fluxes. *J. Geophys. Res.*, **106**(C8), 16,729–16,745.
- McMillen, R.T. 1988. An eddy correlation technique with extended applicability to non-simple terrain. *Bound.-Layer Meteorol.*, **43**(3), 231–245.
- Maslanik, J.A., C. Fowler, J. Stroeve, S. Drobot and H.J. Zwally. 2007. A younger, thinner Arctic ice cover: increased potential for rapid, extensive ice loss. *Geophys. Res. Lett.*, **34**(24), L24501. (10.1029/2007GL032043.)
- Massman, W.J. and X. Lee. 2002. Eddy covariance flux corrections and uncertainties in long-term studies of carbon and energy exchanges. *Agric. Forest Meteorol.*, **113**(1–4), 121–144.
- Miller, L.A. and 9 others. In press. Carbon dynamics in sea ice: a winter flux time series. *J. Geophys. Res.* (10.1029/2009JC00605844.)
- Mock, T. and 7 others. 2002. Micro-optodes in a sea ice: a new approach to investigate oxygen dynamics during sea ice formation. *Aquat. Microbial Ecol.*, **29**(3), 297–306.

- Moncrieff, J.B., Y. Malhi and R. Leuning. 1996. The propagation of errors in long-term measurements of land-atmosphere fluxes of carbon and water. *Global Change Biol.*, **2**(3), 231–240.
- Mundy, C.J. 2003. Biological and oceanographic sampling. In Mundy, C.J. and D.G. Barber, eds. *C-ICE'02 Field Summary*. Winnipeg, Man., University of Manitoba. Centre for Earth Observation Science, 56–61.
- Mundy, C.J., D.G. Barber and C. Michel. 2005. Variability of snow and ice thermal, physical and optical properties pertinent to sea ice algae biomass during spring. *J. Mar. Systems*, **58**(3–4), 107–120.
- Nghiem, S.V., I.G. Rigor, D.K. Perovich, P. Clemente-Colón, J.W. Weatherly and G. Neumann. 2007. Rapid reduction of Arctic perennial sea ice. *Geophys. Res. Lett.*, **34**(19), L19504. (10.1029/2007GL031138.)
- Nomura, D., H. Yoshikawa-Inoue and T. Toyota. 2006. The effect of sea-ice growth on air–sea CO₂ flux in a tank experiment. *Tellus B*, **58**(5), 418–426.
- Ono, K., A. Miyata and T. Yamada. 2008. Apparent downward CO₂ flux observed with open-path eddy covariance over a non-vegetated surface. *Theor. Appl. Climatol.*, **92**(3–4), 195–208.
- Papadimitriou, S., H. Kennedy, G.S. Dieckmann and D.N. Thomas. 2003. Experimental evidence for carbonate precipitation and CO₂ degassing during sea ice formation. *Geochim. Cosmochim. Acta*, **68**(8), 1749–1761.
- Perovich, D.K., J.A. Richter-Menge, K.F. Jones and B. Light. 2008. Sunlight, water, and ice: extreme Arctic sea ice melt during the summer of 2007. *Geophys. Res. Lett.*, **35**(11), L11501. (10.1029/2008GL034007.)
- Pomeroy, J.W., T.D. Davies, H.G. Jones, P. Marsh, N.E. Peters and M. Tranter. 1999. Transformations of snow chemistry in the boreal forest: accumulation and volatilization. *Hydrol. Process.*, **13**(14–15), 2257–2273.
- Prytherch, J., M.J. Yelland, R.W. Pascal, B.I. Moat, I. Skjelvan and C.C. Neill. 2010. Direct measurements of the CO₂ flux over the ocean: development of a novel method. *Geophys. Res. Lett.*, **37**(3), L03607. (10.1029/2009GL041482.)
- Riedel, A., C. Michel, M. Gosselin and B. LeBlanc. 2008. Winter–spring dynamics in sea-ice carbon cycling in the coastal Arctic Ocean. *J. Mar. Systems*, **74**(3–4), 918–932.
- Rothrock, D.A., D.B. Percival and M. Wensnahan. 2008. The decline in arctic sea-ice thickness: separating the spatial, annual, and interannual variability in a quarter century of submarine data. *J. Geophys. Res.*, **113**(C5), C05003. (10.1029/2007JC004252.)
- Rysgaard, S., R.N. Glud, M.K. Sejr, J. Bendtsen and P.B. Christensen. 2007. Inorganic carbon transport during sea ice growth and decay: a carbon pump in polar seas. *J. Geophys. Res.*, **112**(C3), C03016. (10.1029/2006JC003572.)
- Rysgaard, S., J. Bendtsen, L.T. Pedersen, H. Ramløv and R.N. Glud. 2009. Increased CO uptake due to sea ice growth and decay in the Nordic Seas. *J. Geophys. Res.*, **114**(C9), C09011. (10.1029/2008JC005088.)
- Semiletov, I., A. Makshtas, S.-I. Akasofu and E.L. Andreas. 2004. Atmospheric CO balance: the role of Arctic sea ice. *Geophys. Res. Lett.*, **31**(5), L05121. (10.1029/2003GL017996.)
- Serrano-Ortiz, P., A.S. Kowalski, F. Domingo, B. Ruiz and L. Alados-Arboledas. 2008. Consequences of uncertainties in CO₂ density for estimating net ecosystem CO₂ exchange by open-path eddy covariance. *Bound.-Layer Meteorol.*, **126**(2), 209–218.
- Serreze, M.C. and J.A. Francis. 2006. The Arctic amplification debate. *Climatic Change*, **76**(3–4), 241–264.
- Sullivan, P.F., J.M. Welker, S.J.T. Arens and B. Sveinbjörnsson. 2008. Continuous estimates of CO₂ efflux from arctic and boreal soils during the snow-covered season in Alaska. *J. Geophys. Res.*, **113**(G4), G04009. (10.1029/2008JG000715.)
- Thomas, D.N. and G.S. Dieckmann, eds. 2010. *Sea ice. Second edition*. Oxford, Wiley-Blackwell.
- Thomas, D.N., S. Papadimitriou and C. Michel. 2010. Biogeochemistry of sea ice. In Thomas, D.N. and G.S. Dieckmann, eds. *Sea ice. Second edition*. Oxford, Wiley-Blackwell.
- Tison, J.L., C. Haas, M.M. Gowing, S. Sleewaegen and A. Bernard. 2002. Tank study of physico-chemical controls on gas content and composition during growth of young sea ice. *J. Glaciol.*, **48**(161), 177–191.
- Tison, J.-L. and 8 others. 2008. Temporal evolution of decaying summer first-year sea ice in the Western Weddell Sea, Antarctica. *Deep-Sea Res. II*, **55**(8–9), 975–987.
- Webb, E.K., G.I. Pearman and R. Leuning. 1980. Correction of flux measurements for density effects due to heat and water vapour transfer. *Q. J. R. Meteorol. Soc.*, **106**(447), 85–100.
- Yang, P.C., T.A. Black, H.H. Neumann, M.D. Novak and P.D. Blanken. 1999. Spatial and temporal variability of CO₂ concentration and flux in a boreal aspen forest. *J. Geophys. Res.*, **104**(D22), 27,653–27,661.
- Zeebe, R.E. and D. Wolf-Gladrow. 2001. *CO₂ in seawater: equilibrium, kinetics, isotopes*. Amsterdam, Elsevier.
- Zemmelink, H.J., B. Delille, J.L. Tison, E.J. Hintsa, L. Houghton and J.W.H. Dacey. 2006. CO₂ deposition over the multi-year ice of the western Weddell Sea. *Geophys. Res. Lett.*, **33**(13), L13606. (10.1029/2006GL026320.)